Atmospheric Oxidation of Toluene in a Large-Volume Outdoor Photoreactor: In Situ Determination of Ring-Retaining Product Yields

Björn Klotz, Søren Sørensen, Ian Barnes,* and Karl H. Becker

Bergische Universität, Physikalische Chemie - FB 9, Gaussstrasse 20, D-42097 Wuppertal, Germany

Thomas Etzkorn, Rainer Volkamer, and Ulrich Platt

Universität Heidelberg, Institut für Umweltphysik, Im Neuenheimer Feld 366, D-69120 Heidelberg, Germany

Klaus Wirtz and Montserrat Martín-Reviejo

Fundación Centro de Estudios Ambientales del Mediterraneo (CEAM), Parque Tecnológico, Calle 4, Sector Oeste, E-46980 Paterna (Valencia), Spain

Experiments on the photooxidation of toluene/NO_x/air mixtures were performed in the European Photoreactor (EUPHORE), a large-scale outdoor reaction chamber located in Valencia/Spain. The objective of the study was the in situ determination of the yields of ring-retaining products by differential optical absorption spectroscopy (DOAS) and the elucidation of their formation pathways. The experiments were performed with toluene concentrations between 0.68 and 3.85 ppm and initial NO_x concentrations ranging from 3 to 300 ppb, i.e., down to the range actually observed in the lower atmosphere. The ring-retaining product yields were found to be $5.8 \pm 0.8\%$, $12.0 \pm 1.4\%$, $2.7 \pm 0.7\%$, and $3.2 \pm 0.6\%$ for benzaldehyde, *o*-cresol, *m*-cresol, and *p*-cresol, respectively. Under the experimental conditions, no dependency of the yields on the NO_x concentration or the toluene/NO_x ratio could be found. The formation kinetics of the cresols are in line with a "prompt" formation mechanism, i.e., abstraction of a hydrogen atom from the toluene−OH adduct (toluene−OH + O_2 → cresols + HO_2). In addition, substantial evidence was found that reaction with NO_3 radicals represents an important sink for cresols in smog chamber studies conducted under conditions of NO_x concentrations above the range observed in the troposphere, possibly also under tropospheric conditions.

Introduction

In urban and industrial areas large amounts of aromatic hydrocarbons are emitted into the atmosphere, predominantly from anthropogenic sources such as fossil fuel burning and solvent use.[1] In the presence of NO_x (NO + NO_2), the degradation of these compounds in the troposphere ultimately leads to the formation of ozone and other photooxidants in these areas.[2,3] Because of their reactivity and the amounts emitted, aromatic hydrocarbons are regarded as the most important class of hydrocarbons with regard to photooxidant formation in urban air.[4]

Among the aromatic hydrocarbons, toluene is the most abundant species found in the urban atmosphere, making it the most important single compound with regard to photooxidant formation.[4] Predictions such as this, however, are based on model calculations which rely heavily on the correctness of the input data, i.e., the chemical mechanisms describing the degradation of the various hydrocarbons and emission inventories. The chemical degradation of toluene and other aromatic hydrocarbons is known to proceed almost exclusively via reaction with OH radicals.[3,5] For toluene, two pathways are operative. Abstraction of a hydrogen atom from the methyl group accounts for less than 10% of the total, with the remainder being addition of OH to the aromatic ring[3,5] resulting in the

formation of a methyl-hydroxy-cyclohexadienyl radical,[6,7] hereafter termed toluene−OH adduct. Under atmospheric conditions, the toluene−OH adduct will react predominantly with molecular oxygen.[8] In this reaction, an important and particularly debated uncertainty exists in the exact yield of hydroxylated aromatics, i.e., cresols in the case of toluene. Various recent studies have come to significantly different conclusions, ranging from negligible yields[9] to extremely high values,[10] with two studies obtaining values intermediate between these extremes.[11,12] A detailed overview of cresol yields published in the literature is given below. One drawback with these studies is the fact that the compounds were not detected in situ but indirectly by GC-FID or HPLC. Although these indirect methods are very sensitive, they necessitate the employment of sampling and sample preparation techniques which may lead to unintentional errors being made such as the possible formation or destruction of highly reactive sample compounds such as cresols. These difficulties may help to explain the large discrepancies between the various studies. Such errors can be avoided when absolute measurement techniques such as DOAS (differential optical absorption spectroscopy)[13,14] or FT-IR (Fourier transform infrared) spectroscopy[15] are employed whose accuracy solely depends on the correctness of the absorption cross sections used for the evaluation of the spectra. With these methods, no calibration of apparatus is needed. They both have been successfully employed in previous studies performed in the European Photoreactor (EUPHORE).[16,17] DOAS is a

---

* Author to whom correspondence should be addressed. Fax: xx49-202/ 439-2505. E-mail: barnes@physchem.uni-wuppertal.de.

particularly sensitive technique for the detection of aromatic hydrocarbons.[18] In previous studies using DOAS for the detection of aromatic hydrocarbons reliable quantification was difficult due to absorptions of O_2 which significantly interfere with those of aromatic hydrocarbons. This difficulty has recently been resolved by Volkamer et al.,[19] who measured high-resolution reference spectra of molecular oxygen. The difficulties with the determination of accurate gas-phase absorption cross sections, especially for the highly reactive and nonvolatile cresols, were also recently overcome by calibrations performed at low concentrations in a large-volume cell.[20]

One problem in some previous smog-chamber studies[11,21] was the influence of the very high NO_2 concentrations of several ppm usually employed. It is known that the toluene−OH adduct initially formed from the addition of the OH radical to the aromatic ring rapidly reacts with NO_2, compared to a very slow reaction with O_2.[8] Under smog-chamber conditions when NO_2 concentrations reach ppm levels, reaction with NO_2 becomes a significant removal process for the toluene−OH adduct. Though product data for this reaction are not available, it is assumed that high NO_2 concentrations lead to higher yields of the cresol isomers.[9,11,22]

In this study, the yields of the ring-retaining products benzaldehyde and *o*-, *m*-, and *p*-cresol have been determined by an in situ method at NO_x concentrations close to those observed in the troposphere of urban areas. This, in conjunction with the facts that real sunlight could be used for the photooxidation and that the experiments were conducted in a large-volume chamber, has resulted in a reliable determination of the ring-retaining products from the oxidation of toluene which can be used in chemical models used to describe tropospheric photooxidation formation.

Experimental Section

All experiments were performed in the European Photoreactor (EUPHORE), a large-volume outdoor smog chamber integrated into the Centro de Estudios Ambientales del Mediterraneo (CEAM) in Valencia/Spain. EUPHORE consists of two half-spherical FEP (fluorine ethene propene) chambers mounted on aluminum floor panels covered with FEP foil. This foil is highly transparent even to short-wavelength sunlight, with transmissions ranging from 85 to 90% in the range 500−320 nm to >75% at 290 nm. To avoid unwanted heating of the chamber, the aluminum floor panels are fitted with an active cooling system designed to keep their temperature constant even during long-term irradiations in summertime, allowing realistic atmospheric temperature conditions to be maintained. The chamber used for the experiment described here has a volume of ca. 170 m^3, two ventilators with a throughput of 67 m^3 min^{-1} each are installed to ensure homogeneous reaction mixtures. To supply the chambers with hydrocarbon and NO_y-free dry air, an air-drying and purification system is installed which is able to reduce the nonmethane hydrocarbon content to levels below 0.3 μg m^{-3}. When not in use, the chambers are protected by hydraulically operated steel housings.

In the chamber where the experiments were performed, two White mirror systems are installed on the aluminum floor panels, one for the FT-IR and one for the DOAS system. The FT-IR, a NICOLET Magna 550 with an MCT detector and a resolution of 1 cm^{-1}, was operated at an optical path length of 326.8 m. The DOAS, constructed and operated by the group from University of Heidelberg, was operated at a short optical path of 128 m to allow the simultaneous detection of reactants and products. The mirrors of the FT-IR White system are gold

```
RE1:TOL+OH=BALD+OH;A=0.411D-12
RE2:TOL+OH=OCRE+OH;A=0.697D-12
RE3:TOL+OH=MCRE+OH;A=0.149D-12
RE4:TOL+OH=PCRE+OH;A=0.173D-12
RE5:TOL+OH=PROD+OH;A=4.53D-12
* total k(OH+toluene) = 5.96D-12 cm3 s-1

RE6:BALD+OH=PROD+OH;A=12.9D-12
RE7:OCRE+OH=PROD+OH;A=42D-12
RE8:MCRE+OH=PROD+OH;A=64D-12
RE9:PCRE+OH=PROD+OH;A=47D-12
* Atkinson, J Phys Chem Ref Data, Monograph No. 2, 1994

RE10:TOL=LEAK;A=0.75D-5
RE11:BALD=LEAK;A=0.75D-5
RE12:OCRE=LEAK;A=0.75D-5
RE13:MCRE=LEAK;A=0.75D-5
RE14:PCRE=LEAK;A=0.75D-5
* dilution rates as determined by SF6-decay

RE15:DU0=DU1;A=8D-4
RE16:DU1=DU2;A=8D-4
RE17:DU2=OH+DU3+DU3;A=0.25D-3
RE18:DU3=DU4;A=8D-3
RE19:DU4=DU5;A=8D-3
RE20:DU5+OH=PROD;A=10.15D-11
* dummy reactions to adjust OH to toluene decay

CON(TOL)=1.777D13
CON(DU0)=50D6
CON(BALD)=0D9
CON(OCRE)=0D9
CON(MCRE)=0D9
CON(PCRE)=0D8
* initial concentrations
```

Figure 1. Example of the chemical mechanism used in the simulations of the concentration−time profiles of ring-retaining products from toluene, for explanation see text. TOL, toluene; BALD, benzaldehyde; OCRE, *o*-cresol; MCRE, *m*-cresol; PCRE, *p*-cresol; PROD, products; CON, initial concentrations.

coated, while the DOAS mirrors are aluminum coated and have an additional coating (Allflex-UV, Balzers, Liechtenstein) to enhance their reflectivity in the UV spectral range. The DOAS consists of a *f*/6.9 Czerny-Turner spectrograph (Acton Spectra Pro 500) with a focal length of 0.5 m. For the experiments presented here, a 1200 gr mm^{-1} grating was used, corresponding to a dispersion of 0.038 nm $pixel^{-1}$. The spectral resolution, defined as the fwhm (full width at half-maximum) of an atomic emission line, was 0.22 nm. For most experiments, the detector was a photodiode array (Hoffmann, Rauenberg), which was cooled to −20 °C to reduce the dark current of the diodes. In the first experiment conducted, see Figure 2, a photodiode array developed at the University of Heidelberg was used which was cooled to −30 °C. A detailed description of the DOAS system used is given in the literature.[23] The absorption cross sections used for the evaluation of the DOAS and FT-IR spectra were determined in a separate study.[20]

In addition to these instruments, two $J(NO_2)$ filter radiometers (one measuring direct sunlight, one facing downward to measure reflected light from the floor panels) and sampling ports for an ozone monitor (Monitor Labs), a Monitor Labs ML9841A NO_x monitor with a catalytic converter and an Eco Physics CLD 770 AL NO_x monitor with a photolytic converter PLC 760 are installed. The temperature in the chamber was measured with two thermocouples PT-100, one measuring the floor temperature and one measuring the temperature of the chamber air. The ozone, NO_x, temperature, and radiation measurement data were collected and saved by a data acquisition system. A detailed description of the European Photoreactor EUPHORE can be found in the literature.[23]

Toluene was added to the chamber by gently heating the required amount in a stream of nitrogen entering the chamber,

Oxidation of Toluene in an Outdoor Photoreactor

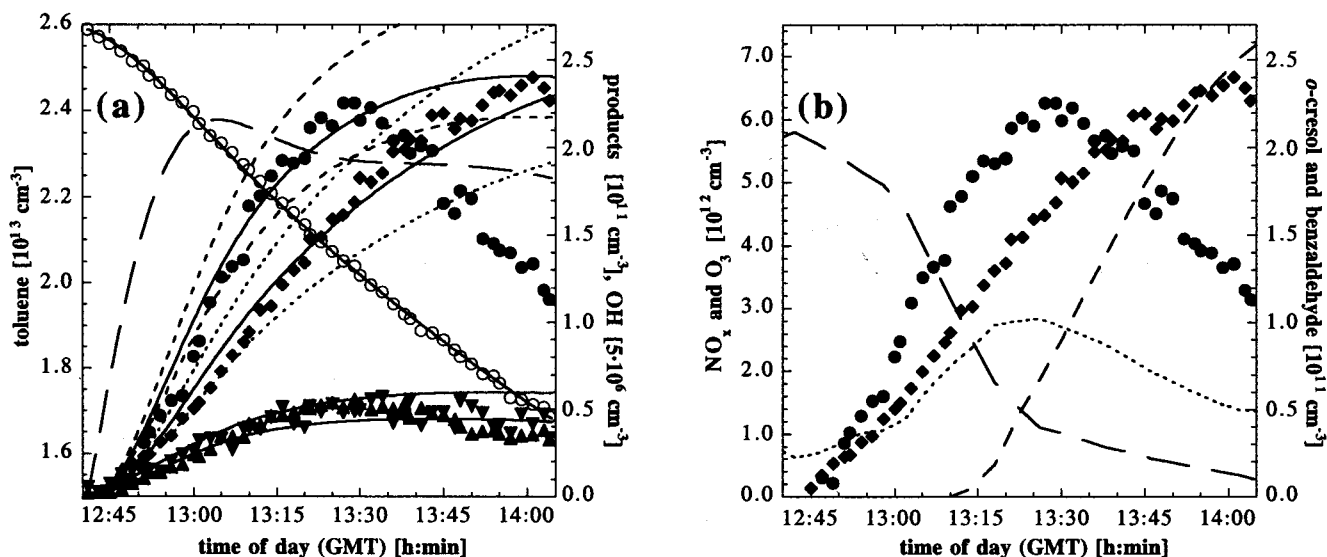*J. Phys. Chem. A, Vol. 102, No. 50, 1998* **10291**

Figure 2. Concentration−time profiles of a toluene/NO photooxidation experiment (1050 ppb toluene, 230 ppb NO). (a) Experimental and simulated concentration−time profiles of toluene (left scale), benzaldehyde, the cresols, and OH (all right scale). Lines denote the simulated profiles, dotted lines represent the error limits of the simulations, and symbols are experimental data. The long dashed line represents the calculated OH-radical concentrations. (b) Comparison of the c/t-profiles of benzaldehyde and o-cresol to those of NO (long dashed line), NO_2 (dotted line), and ozone (dashed line). Symbols: (○) toluene, (◆) benzaldehyde, (●) o-cresol, (▼) m-cresol, (▲) p-cresol.
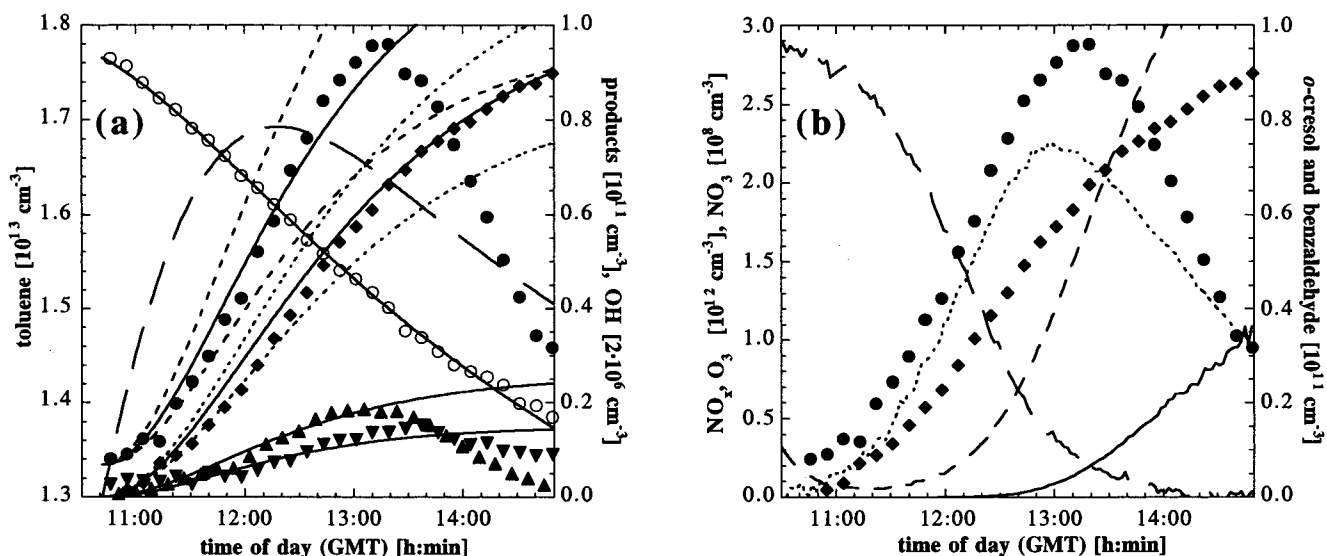

Figure 3. Concentration−time profiles of a toluene/NO photooxidation experiment (730 ppb toluene, 115 ppb NO). Graph (b) also includes the calculated concentration−time profile of NO_3 (solid line), legend otherwise same as for Figure 2.

and NO was injected into the same stream through a septum. After allowing some time for mixing of the compounds, the photooxidation was initiated by opening the protective housings and exposing the chamber to sunlight. Due to small cracks in the FEP foil and the pressure necessary to keep the chamber inflated, most experiments had a leak rate of ca. 3% h^{-1}. To accurately determine this dilution rate, ca. 20 ppb of SF_6 (1 ppm = 2.46×10^{13} cm^{-3} at 1013 mbar and 298 K) was added as an inert tracer substance in most experiments. The decay of SF_6 was monitored using its very intense IR absorption band centered around 950 cm^{-1}. In the experiments where no SF_6 was added, the dilution rate was calculated from the loss of toluene in darkness prior to exposing the chamber to sunlight.

Method of Evaluation. The concentration−time profiles of toluene and its oxidation products were evaluated by computer-aided simulation of the profiles using a greatly simplified chemical mechanism. In these simulations, the OH radical concentration was adjusted to describe the measured toluene

decay in the experiments. Reaction with OH radicals was assumed to be the sole chemical loss process of toluene and its ring-retaining oxidation products. In addition, losses through chamber leaks were taken into account. The limitations of these assumptions will be discussed in detail below. The chemical simulation program ChemSimul developed at the Danish national research facility at Risø was used for the calculations.

As an example for the mechanism used, Figure 1 shows the relevant parts of the input file for the experiment depicted in Figure 4. The OH radical concentrations are controlled through reactions RE15−RE20. The initial formation of OH results from RE17, after two intermediate steps, RE15 and RE16. After two additional delaying steps, RE18 and RE19, OH is consumed by RE20. The rate constants for RE15−RE20 were adjusted to yield a best fit of the calculated concentration−time profile of toluene to the experimental data. As an additional loss process, dilution through chamber leaks was taken into account by RE10−RE14. Reactions RE6−RE9 represent losses of the
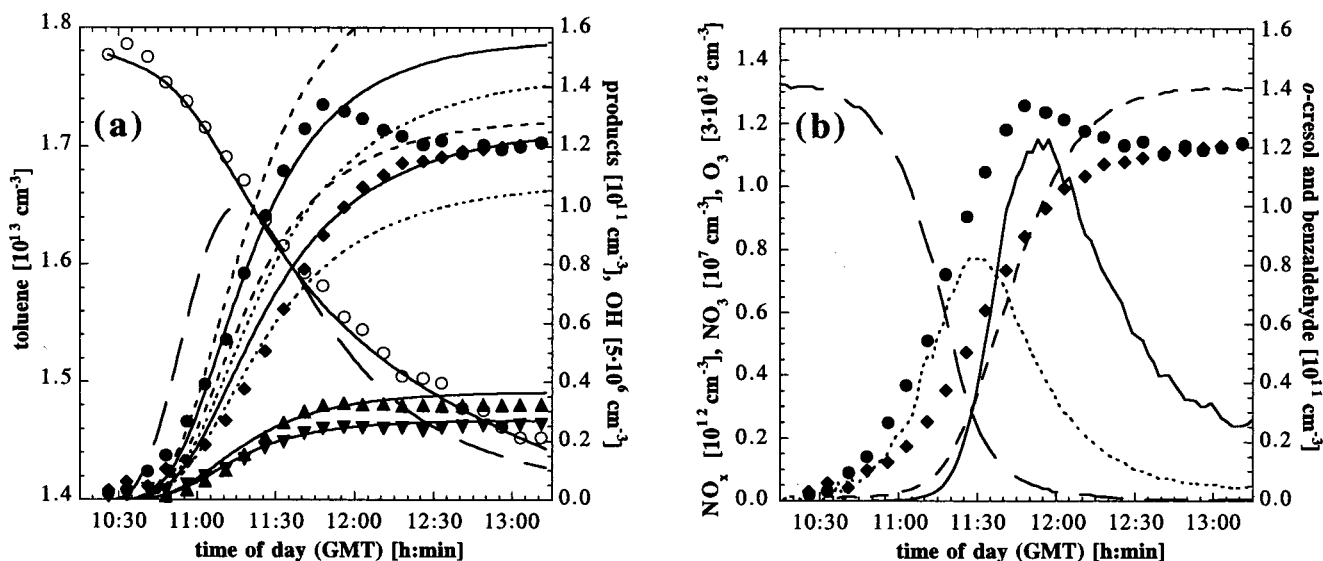
Figure 4. Concentration−time profiles of a toluene/NO photooxidation experiment (725 ppb toluene, 55 ppb NO). Legend same as for Figure 3.

ring-retaining products through reaction with OH radicals, the rate constants are those recommended by Atkinson.[5] The reactions do not consume OH, as its concentration is controlled by reactions RE15−RE20.

Reactions RE1−RE4 are the formation channels of the ring-retaining products observed in the photooxidation of toluene, RE5 is needed to achieve the total OH reaction rate constant of k_{OH}(toluene) = 5.96 × 10^{-12} cm^3 s^{-1} recommended by Atkinson.[5] As is evident from RE1−RE4, the formation of benzaldehyde and the cresols was assumed to result directly from the reaction of OH with toluene, i.e., not through further reaction of a stable intermediate. The delay resulting from the initial formation of a toluene−OH adduct and its subsequent reaction with O$_2$ is negligible at atmospheric partial pressures of O$_2$.
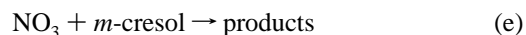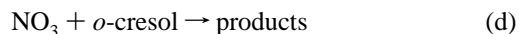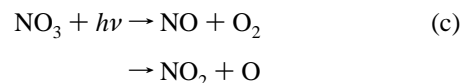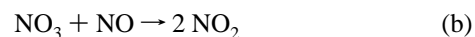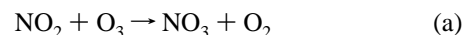
To determine the individual formation yields of the ring-retaining products, the rate constants of their formation channels were adjusted so the simulated concentration−time profiles of the products showed the best possible agreement with the experimental data. Formation yields are then given by the ratios of the individual bimolecular rate constants to the total rate constant of the reaction of toluene with OH radicals. In many experiments, the simplified model was unable to describe the experimental data toward the end of the experiment due to an apparent additional loss of the cresols through reaction with NO$_3$ radicals (see below). In such cases, only the initial formation of the cresols was fitted, before the additional loss process became important.

The error limits given for the product yields calculated in this way represent the range in which the yields could be changed without the simulated concentration−time profiles significantly deviating from the error limits of the experimental values.

In most experiments, the DOAS was used for the determination of both the concentration−time profiles of toluene and its oxidation products. The FT-IR spectrometer available in addition to the DOAS was used to verify the concentration−time profiles of toluene determined by DOAS. In all experiments, both instruments showed identical values within their experimental uncertainties. In the experiments conducted with starting concentrations of toluene around 700 ppb, the toluene concentrations obtained by DOAS were used as ozone absorptions significantly interfered with the FT-IR analysis at these concentrations. In the two experiments conducted at much

higher toluene concentrations of ca. 3.8 ppm, several toluene absorption bands were outside of the applicability of the Lambert−Beer law in the DOAS spectra, necessitating an evaluation at less intense bands, which resulted in a higher error in the concentrations determined. Therefore, and because only a minor ozone interference was observed in the FT-IR spectra at these high toluene concentrations, the FT-IR data were used for toluene in these experiments.

To determine the influence of nitrate radicals on the observed concentration−time profiles, estimates of their concentrations in the various runs were made. For these estimations, a steady state was assumed for NO$_3$, i.e., d[NO$_3$]/dt = 0. From eq 1 below it can be calculated that the formation and degradation rates of NO$_3$ are significantly higher than their quotient, making the assumption of a steady state valid. The following reactions were taken into account:

$$NO_2 + O_3 \rightarrow NO_3 + O_2 \qquad \text{(a)}$$

$$NO_3 + NO \rightarrow 2 NO_2 \qquad \text{(b)}$$

$$NO_3 + h\nu \rightarrow NO + O_2 \qquad \text{(c)}$$

$$\rightarrow NO_2 + O$$

$$NO_3 + o\text{-cresol} \rightarrow \text{products} \qquad \text{(d)}$$

$$NO_3 + m\text{-cresol} \rightarrow \text{products} \qquad \text{(e)}$$

$$NO_3 + p\text{-cresol} \rightarrow \text{products} \qquad \text{(f)}$$

Since the total decomposition rate of NO$_3$ is only insignificantly different from its formation rate, the NO$_3$ concentration can be calculated by eq 1:

$$[NO_3] = \frac{k_a[O_3][NO_2]}{k_b[NO] + k_c + k_d[o\text{-cresol}] + k_e[m\text{-cresol}] + k_f[p\text{-cresol}]} \qquad (1)$$

The equilibrium NO$_3$ + NO$_2$ ⇌ N$_2$O$_5$ need not be considered in this calculation, since under the steady-state assumption the rates of the forward and reverse reactions are equal and cancel each other out. The photolysis frequencies of NO$_3$ radicals
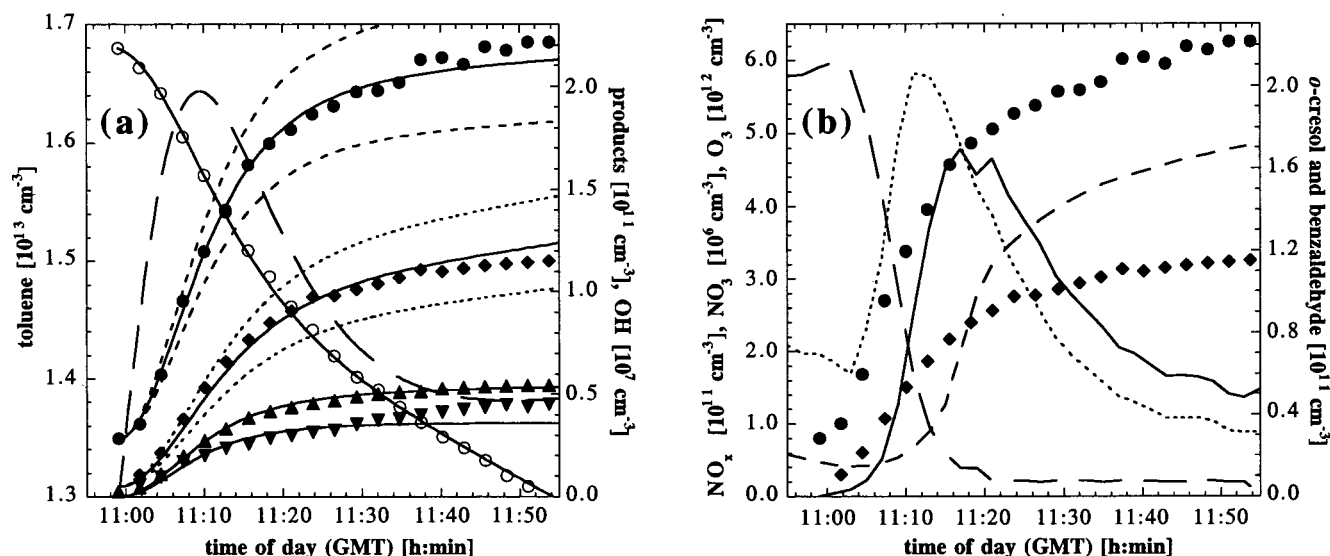
Oxidation of Toluene in an Outdoor Photoreactor

J. Phys. Chem. A, Vol. 102, No. 50, 1998 **10293**

Figure 5. Concentration−time profiles of a toluene/NO photooxidation experiment (690 ppb toluene, 24 ppb NO). Legend same as for Figure 3.
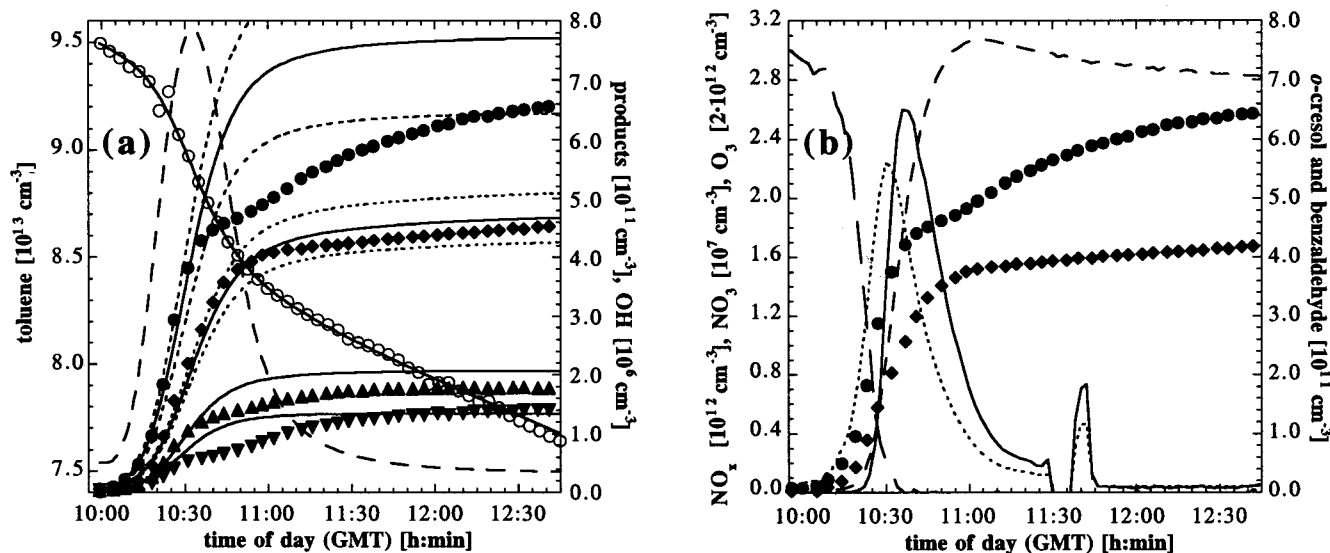

Figure 6. Concentration−time profiles of a toluene/NO photooxidation experiment (3850 ppb toluene, 120 ppb NO). Legend same as for Figure 3.

(reaction c) could not be measured directly in the EUPHORE chamber, therefore an approximation was used for their determination. They were calculated relative to the photolysis frequencies of NO_2, which were measured with a filter radiometer. A conversion factor was estimated based on the highest NO_2 photolysis frequency measured in the experiments performed, which was at 11:40 h in the experiment displayed in Figure 6. For that time and day, a corresponding NO_3 photolysis frequency was calculated based on the data of Orlando et al.[24] Additional correction factors were incorporated to account for absorption of sunlight by the FEP foil and for the albedo of the aluminum floor panels of the chamber. Another requirement of this approach is that the scattering of light in the region around 630 nm, where NO_3 radicals photolyze, must be very similar to the scattering of light around 400 nm, where NO_2 absorbs, which is not necessarily true in all cases. The errors introduced into the calculated NO_3 concentrations by these uncertainties are, however, very small, as the major degradation pathway of the NO_3 radicals is the reaction with NO, not photolysis. Typically, the reaction with NO was found to be 10−50 times faster than photolysis.

The NO_3 concentrations calculated in this way may, however, only be regarded as upper limits. The true NO_3 concentration will be lower, as some sinks could not be included in the calculation. These are notably reaction with peroxyl radicals and other (nonradical) intermediates in the photooxidation of aromatic hydrocarbons.

Results and Discussion

A total of nine experiments were performed. The initial conditions of these experiments are listed in Table 1, together with the formation yields of the ring-retaining products benzaldehyde and *o*-, *m*-, and *p*-cresol obtained from simulations as described above. The individual experiments are not ordered chronologically, but by their initial toluene/NO ratios, with experiments where NO_x concentrations were kept constant added at the end.

The averaged yields from Table 1 are 5.8 ± 0.8% for benzaldehyde and 12.0 ± 1.4%, 2.7 ± 0.7%, and 3.2 ± 0.6% for *o*-, *m*-, and *p*-cresol, respectively. Within their experimental uncertainties, the yields are dependent neither on the NO_x concentration nor on the initial toluene/NO ratio. This behavior might have been expected as the NO_2 concentration is suf-

TABLE 1: Overview of the Initial Conditions and Results of the Experiments Presented in This Study

experiment in figure	initial conditions		product yields				
	c_0(toluene) [ppb]	c_0(NO) [ppb]	benzaldehyde [%]	*o*-cresol [%]	*m*-cresol [%]	*p*-cresol [%]	all cresols [%]
2	1050	230	5.9 ± 1.0	10.7 ± 2.0	2.7 ± 1.5	2.9 ± 1.0	16.3 ± 2.7
3	730	115	6.6 ± 1.0	10.6 ± 2.5	1.6 ± 1.5	2.3 ± 1.0	14.5 ± 3.1
4	725	55	6.9 ± 1.0	11.7 ± 2.0	2.5 ± 1.5	2.9 ± 1.0	17.1 ± 2.7
5	690	24	5.4 ± 1.0	13.9 ± 2.0	3.2 ± 1.5	3.9 ± 1.0	21.0 ± 2.7
6	3850	120	5.6 ± 0.5	12.1 ± 2.0	2.5 ± 1.5	3.4 ± 1.0	18.0 ± 2.7
7	3800	28	4.9 ± 0.7	10.2 ± 1.5	2.2 ± 1.5	2.8 ± 1.0	15.2 ± 2.3
8	680	$3-3.5$ const[a]	4.7 ± 1.0	13.4 ± 2.0	4.0 ± 1.5	3.5 ± 1.0	20.9 ± 2.7
9	725	$8.5-12$ const[a]	5.7 ± 1.0	13.4 ± 2.0	2.7 ± 1.5	3.9 ± 1.0	20.0 ± 2.7
10	710	300 const[b]	6.9 ± 1.0	*14.8 ± 2.0*	*2.3 ± 1.5*	*3.5 ± 1.0*	*20.6 ± 2.7*
	average yields		5.8 ± 0.8	12.0 ± 1.4	2.7 ± 0.7	3.2 ± 0.6	17.9 ± 2.5

[a] In these experiments, the total concentration of NO_x was kept at constant levels of $3-3.5$ and $8.5-12$ ppb, respectively. [b] In this experiment, a constant NO concentration of ca. 300 ppb was maintained. The cresol yields in this experiment might have been influenced by the high NO_2 concentrations which accumulated; they were therefore not included in the calculation of the average yields.

TABLE 2: Comparison of the Formation Yields of *o*-Cresol and Benzaldehyde Obtained in This Study to Literature Values

literature	experimental conditions, methods	yields	
		benzaldehyde [%]	*o*-cresol [%]
Atkinson et al. 1980 (25)	NO_x, solar simulator, GC/FID	12	21
Atkinson et al. 1983 (26)	CH_3ONO/NO, solar simulator, GC/FID	7.3 ± 2.2	13.1 ± 7.2
Shepson et al. 1984 (27)	CH_3ONO/NO, blacklamps, HPLC	5.4	
Bandow et al. 1985 (28)	NO_x, blacklamps, FTIR	11 ± 1	
Gery et al. 1985 (29)	HONO, UV fluorescent lamps, GC/FID	10.4 ± 2.9	22
Leone et al. 1985 (30)	NO_x, sunlight, GC/FID	7.1	16
Atkinson et al. 1989 (22)	NO_x, blacklamps, GC/FID	6.5 ± 0.8	20.4 ± 2.7
Seuwen and Warneck 1996 (10)	$2 + 10$ l cells, H_2O_2/UV lamps, 1000 ppm H_2O_2 and toluene, GC/FID and HPLC	5.3 ± 1.1	38.5 ± 8.3
Bierbach et al. 1994 (9)	$400 + 3$ l cells, H_2O_2/UV lamps, 1000 ppm H_2O_2 and toluene, GC/FID	7.0 ± 1.5	up to 23
	1080 l reactor, H_2O_2/UV lamps, GC/FID and FTIR	7.0 ± 1.5	not quantifiable
Atkinson and Aschmann 1994 (11)	alkenes + O_3, GC/FID		12.3 ± 2.2
	CH_3ONO/NO, 1.4 ppm NO_2, blacklamps, GC/FID		14.5 ± 0.7
	CH_3ONO/NO, 7 ppm NO_2, blacklamps, GC/FID		16.0 ± 0.8
Smith et al. 1998 (12)	CH_3ONO/NO, < 1 ppm NO_x, fluorescent bulbs, GC/FID	6.0 ± 0.6	12.3 ± 1.2
this work	toluene/NO, sunlight, DOAS/FTIR	5.8 ± 0.8	12.0 ± 1.4

ficiently low in all the experiments for its reaction with the toluene−OH adduct formed from the initial attack of OH to toluene to be negligible, with the possible exception of the last experiment, see below.

Some of the experiments listed in Table 1 have been independently evaluated by Martín-Reviejo et al.[31] using a different method. The yields obtained by Martín-Reviejo et al. are generally in very good agreement with those obtained in the present study. Since the method of Martín-Reviejo et al. does not take into account losses of reactants and products through dilution of the chamber air, it could only be employed reliably in experiments 8−10. In those experiments, losses of NO_x were compensated by the addition of NO, leading to high OH radical concentrations throughout the experiments (see below). Under these conditions, losses through dilution are small compared to those through OH radical reaction.

A comparison of the formation yields of ring-retaining products obtained in the present study to literature values is given in Table 2. In this table, only the data for *o*-cresol and benzaldehyde are listed, as the database for *m*- and *p*-cresol is very limited. For benzaldehyde, all reported yields are around 7%, with the exception of a few studies from the early eighties.[25,28,29] The result obtained in this work, $5.8 \pm 0.8\%$, is somewhat below this average; however, the values can be regarded as equal within their experimental errors. A very recent study by Smith et al.[12] resulted in a benzaldehyde yield of $6.0 \pm 0.6\%$, almost identical to our value. From the data presented in Table 1, it appears that the benzaldehyde yield is relatively constant regardless of the experimental conditions.

This conjecture is supported by a comprehensive study of Bierbach et al.,[9] in which the yield was investigated over a wide range of experimental conditions.

For the formation yields of *o*-cresol, a different picture emerges. In the eighties, most studies reported yields of around 20% for this compound, albeit with some variations, see for example Atkinson et al.[25] and Atkinson et al.[26] The extremely high value of $38.5 \pm 8.3\%$ recently published by Seuwen and Warneck[10] can be attributed to the experimental conditions of that study, under which a significant influence of heterogeneous reactions is expected. Bierbach et al.[9] obtained similar results under analogous conditions but could show that the *o*-cresol yield is reduced dramatically when the starting concentrations are reduced. Therefore, it seems reasonable to conclude that the results of Seuwen and Warneck[10] are not representative of the troposphere. Bierbach et al.[9] estimated an upper limit of 3% for the yield of *o*-cresol under atmospheric conditions, which is in stark contrast to the value of $12.0 \pm 1.4\%$ obtained in the present study. The discrepancy is almost certainly due to the sampling procedure employed by Bierbach et al.,[9] which consisted of taking gas-phase samples with a glass syringe and injecting them directly into a GC-FID. This procedure probably leads to losses of polar and nonvolatile compounds such as *o*-cresol; these losses could not be quantified. In addition, photolysis of *o*-cresol might have been an additional loss process in their study.

The results of the present study are in excellent agreement with a recent study of Atkinson and Aschmann[11] who found *o*-cresol yields of $12.3 \pm 2.2\%$ under NO_x free conditions and

Oxidation of Toluene in an Outdoor Photoreactor

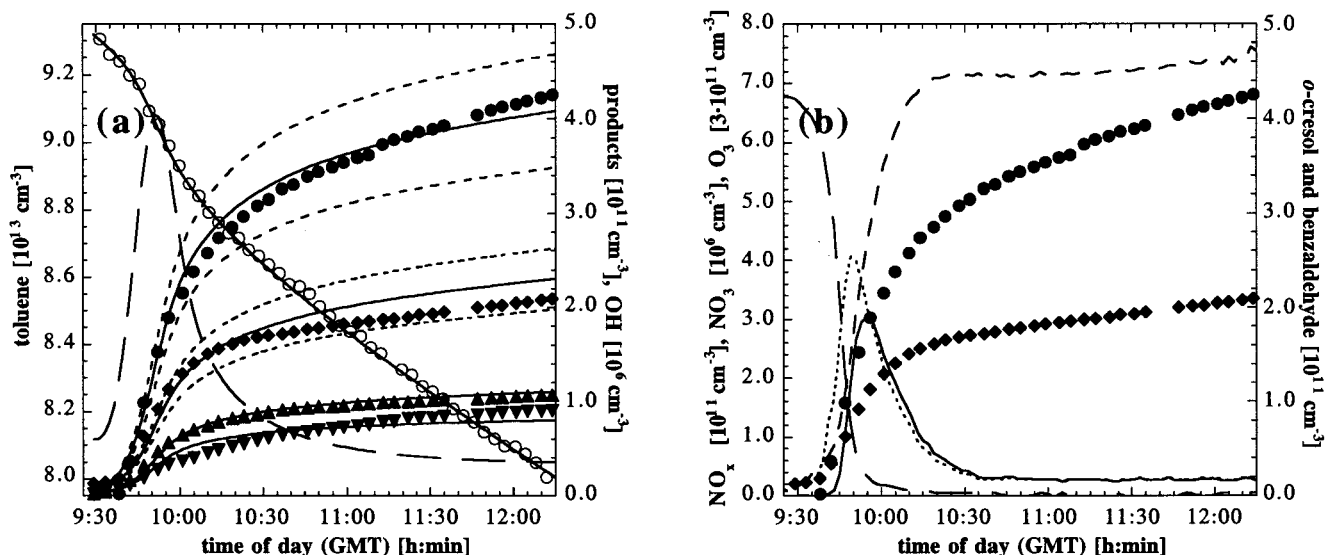*J. Phys. Chem. A, Vol. 102, No. 50, 1998* **10295**

Figure 7. Concentration−time profiles of a toluene/NO photooxidation experiment (3800 ppb toluene, 28 ppb NO). Legend same as for Figure 3.
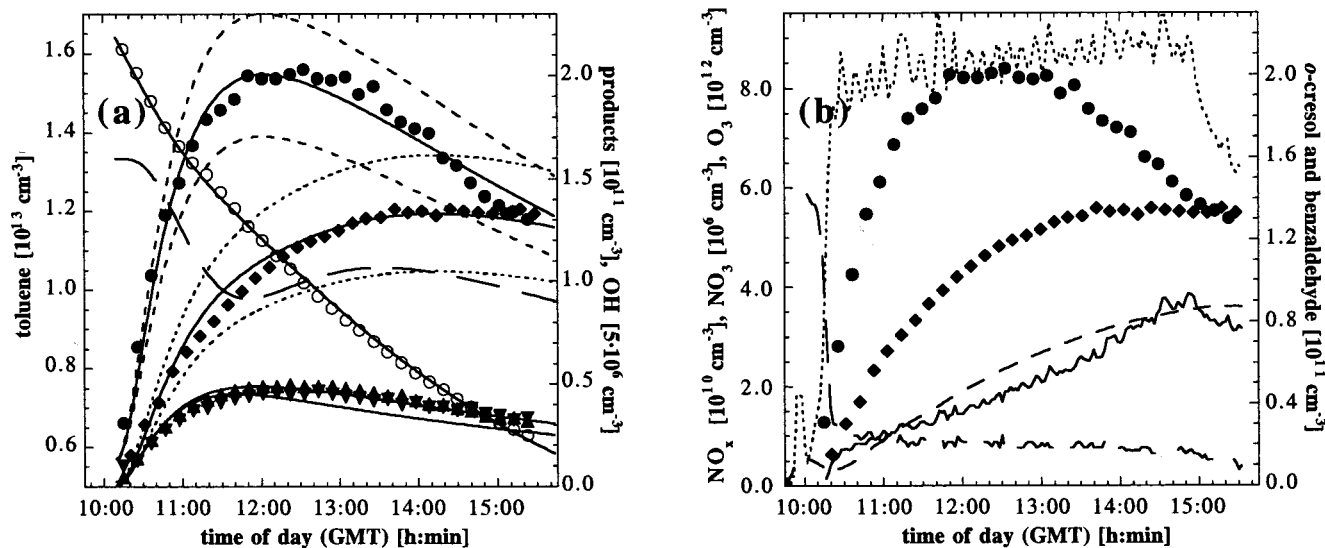

Figure 8. Concentration−time profiles of a toluene/NO photooxidation experiment (680 ppb toluene, 3−3.5 ppb NO_x held constant). Legend same as for Figure 3.

to the results of Smith et al.,[12] who found 12.3 ± 1.2% for *o*-cresol at sub-ppm levels of NO_x. Atkinson and Aschmann[11] found that the *o*-cresol yield rose by several percent in the presence of ppm levels of NO_x. In the present study, only a single experiment (Figure 10) was conducted at NO_x concentrations approaching those employed by Atkinson and Aschmann,[11] this experiment gave the highest measured yield of *o*-cresol with 14.8 ± 2.0%. At an NO_2 concentration of 1.4 ppm, Atkinson and Aschmann found an *o*-cresol yield of 14.5 ± 0.7%, which is again in excellent agreement with our value.

For *m*- and *p*-cresol, which could only be measured as a sum by the chromatographic methods previously employed, yields of 5%[29] and 4.8 ± 0.9%[22] are reported in the literature. This is in reasonable agreement with the value of 5.9 ± 0.9% which can be calculated from the results presented in Table 1. The only study in which *m*- and *p*-cresol were be separated is that of Smith et al.[12] They obtained yields of 2.6 ± 0.3% for *m*-cresol and 3.0 ± 0.3% for *p*-cresol, in good agreement with our data.

The concentration−time profiles obtained in the individual experiments conducted in this study are plotted in Figures 2−10. Each figure consists of two separate plots. The plots marked

as (a), left-hand side of each figure, show experimental and simulated concentration−time profiles of toluene, benzaldehyde, and the cresol isomers as well as the OH radical concentrations calculated from the decay of toluene. Error limits of the simulations are presented only for benzaldehyde and *o*-cresol and not for *m*- and *p*-cresol since these are large and would only complicate the graphs. The plots marked as (b), right-hand side of each figure, show a comparison of the experimental concentration−time profiles of *o*-cresol and benzaldehyde to those of ozone, NO, NO_2, and the estimated NO_3 concentration. The individual experiments will be discussed in the following paragraphs.

In the experiment displayed in Figure 2, a mixture of 1050 ppb toluene and 230 ppb NO was photolyzed. With 4.6, the initial toluene/NO ratio is the lowest of all experiments performed. A simulation as described above resulted in the yields given in Table 1. The concentration−time profile of benzaldehyde is well described over the entire range of Figure 2a. In contrast, the observed concentrations of the cresols become significantly lower than predicted by the simulation toward longer reaction times. This indicates the presence of an additional chemical loss process for the cresols at this time,
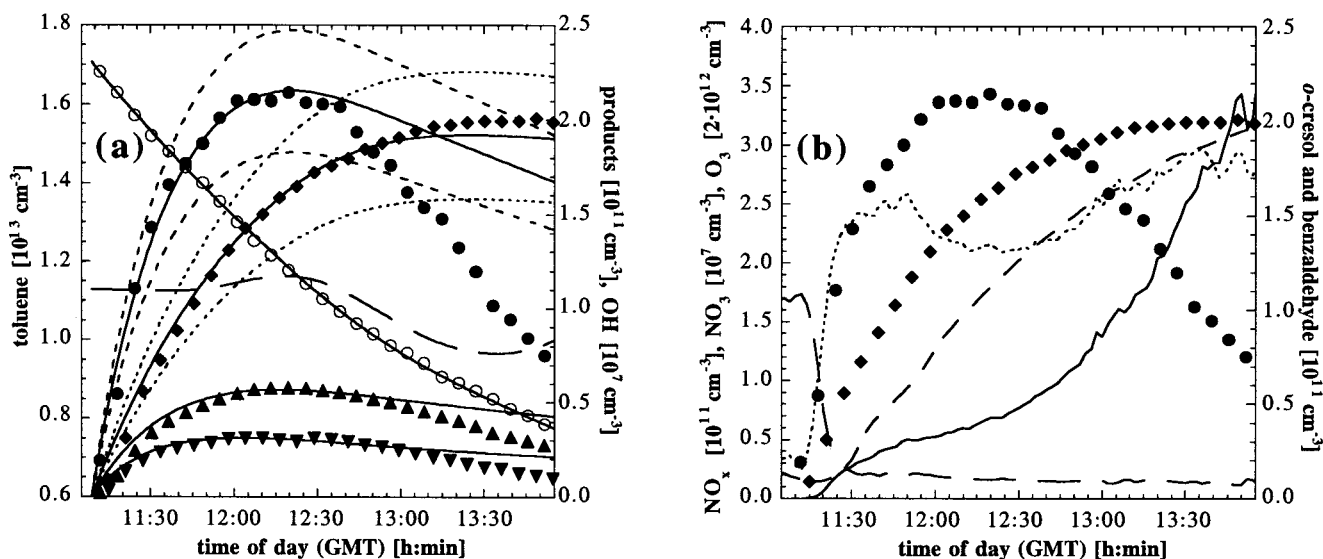
Figure 9. Concentration−time profiles of a toluene/NO photooxidation experiment (725 ppb toluene, 8.5−12 ppb NO_x held constant). Legend same as for Figure 3.
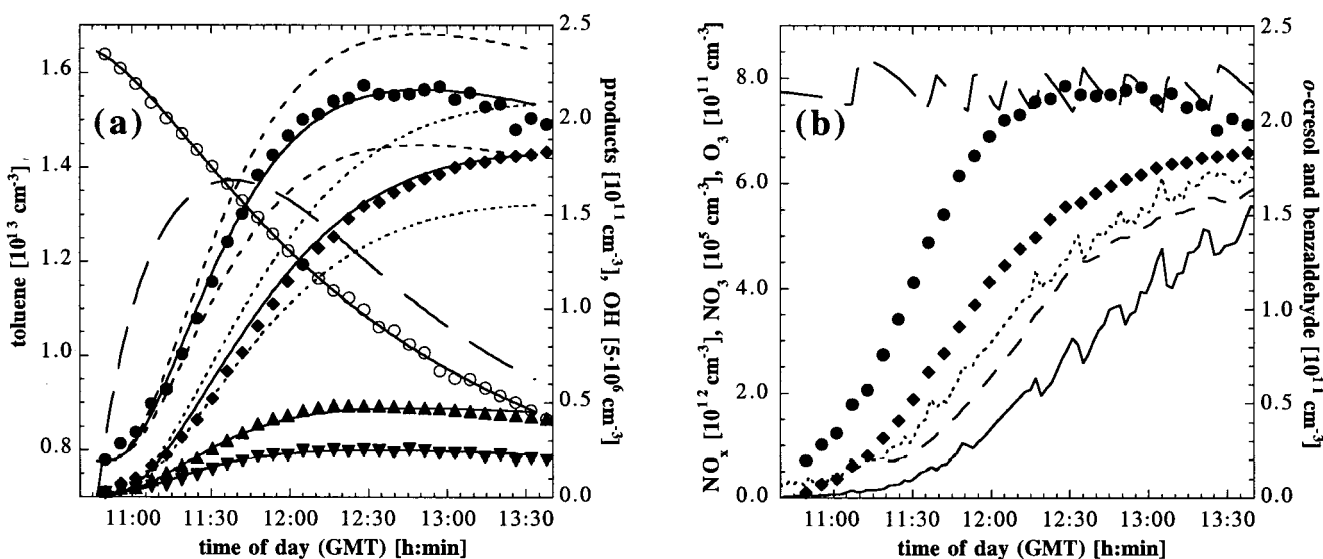

Figure 10. Concentration−time profiles of a toluene/NO photooxidation experiment (710 ppb toluene, 300 ppb NO held constant). Legend same as for Figure 3.

which does not seem to affect benzaldehyde. From Figure 2b it is evident that the losses of cresols occur at the time when NO_2 as well as ozone have accumulated in high concentrations. Under these conditions, NO_3 radicals can be formed. NO_3 radicals are known to react rapidly with cresols,[5] while their reaction with benzaldehyde is almost 4 orders of magnitude slower.[32] The assumption that NO_3 radicals are responsible for the observed losses of the cresols is therefore consistent with the observations. In contrast to the other experiments performed, no estimation of the NO_3 radical concentration could be made here, as only the NO_x analyzer with a catalytic converter was available. The catalytic converter converts not only NO_2 but also several NO_y, notably acetyl peroxynitrate (PAN) and analogous compounds, to NO and measures them as NO_2. An exact knowledge of the NO_2 concentration is, however, a prerequisite for the calculation of NO_3 concentrations (see eq 1).

The experiment shown in Figure 3 was conducted at a slightly higher initial toluene/NO ratio of 6.3, but the starting concentrations were lower, with 730 ppb toluene and 115 ppb NO. The yields calculated from the simulation are again given in Table

1. As expected, the concentration−time profiles of the products show a behavior qualitatively similar to that observed in Figure 2, only the OH radical concentration drops markedly toward the end of the experiment, probably due to the considerably longer reaction time in this experiment. Here, too, the model can only describe the cresol concentrations adequately at the beginning of the experiment, while benzaldehyde is reproduced well even toward the end. Again, the loss of the cresols occurs when conditions exist for the production of NO_3 radicals, namely absence of NO and simultaneous high concentrations of NO_2 and ozone. The NO_3 concentration calculated according to eq 1 starts to become significant at the time the cresol losses start, see Figure 3b. At the end of the experiment, the estimated NO_3 concentration has reached a maximum of almost 5 ppt.

In Figure 4, an experiment with starting concentrations of 725 ppb toluene and 55 ppb NO is shown, the initial toluene/NO ratio has been approximately doubled, it is about 13 here. It is evident in Figure 4a that the concentration−time behavior of benzaldehyde is reproduced well by the simplified chemical mechanism used in the simulation, while for the cresols, a "dip" is observed in their concentrations which cannot be explained

Oxidation of Toluene in an Outdoor Photoreactor

J. Phys. Chem. A, Vol. 102, No. 50, 1998 **10297**

by OH reaction alone. In contrast to the previous experiments, the cresol concentrations do not drop to near zero. This effect is best visible for *o*-cresol, the isomer formed in highest yields. Its concentration stabilizes at ca. 5 ppb. As can be seen in Figure 4b, the maximum decay rate of *o*-cresol corresponds to the maximum of the calculated NO$_3$ radical concentration. The maximum concentration of NO$_3$ is about 1 order of magnitude lower than in the previous experiment. The rapid drop in the NO$_3$ concentration after its maximum is due to the limited availability of NO$_2$ and also its rapid reaction with the cresols, the latter reactions are dominating eq 1 at this point. The almost quantitative loss of NO$_x$ at the end of the experiment is also the probable reason for the drop in the OH radical concentration toward the end of the experiment (see Figure 4a).

Figure 5 shows an experiment with a toluene concentration of 690 ppb, the initial NO concentration was 24 ppb, resulting in an initial toluene/NO ratio of 29, twice as high as in the previous experiment. In this experiment, the concentration–time behavior of both benzaldehyde and the cresols is described well by the simulation, no unexplained loss of cresols is apparent. Such an effect would be expected to occur at the time the NO$_3$ concentration reaches its maximum. The maximum concentration is, however, more than a factor of 2 lower than in the previous experiment. This is apparently too low to have an observable influence on the concentration–time profile of the cresols.

The next two experiments, shown in Figures 6 and 7, have been conducted at significantly higher initial toluene concentrations. This was done mainly to minimize losses of the cresols due to OH radical reaction. In this way, the unknown additional loss process should be more easily distinguishable from the OH reaction.

The first experiment of this type, shown in Figure 6, was performed with initial concentrations of 3850 ppb for toluene and 120 ppb for NO, resulting in an initial toluene/NO ratio of 32. The concentration–time profile of benzaldehyde is described well throughout the experiment, while a "dip" is evident in the profile of the cresols which is not described by the simulation. In Figure 6b, a correlation of these cresol losses with the maximum of the calculated NO$_3$ concentration can be seen. The calculated maximum NO$_3$ concentration is about 1 ppt in this experiment, and thus significantly higher than in the experiment shown in Figure 5. The higher calculated NO$_3$ concentrations can be attributed to the higher NO$_x$ concentrations employed. In contrast to the experiment presented in Figure 4, the cresol concentration not only stabilizes after the NO$_3$ has been consumed, but starts to rise again. This is probably due to the higher concentration of toluene, which acts as an OH radical scavenger. The concentration–time profile of OH exhibits an even sharper maximum as before, probably due to the almost complete loss of NO$_x$ halfway through the experiment. At this time, still existing losses of NO$_x$ appear to be compensated by decomposition of acetyl peroxynitrate (PAN) or analogous compounds. A low but constant NO$_x$ concentration of a few ppb is maintained, leading to a low but constant OH radical concentration of ca. 2×10^5 cm^{-3}. It should be noted that the apparent odd behavior of NO$_x$ and consequently NO$_3$ between 11:30 and 11:45 h is an artifact of maintenance operations at the NO$_x$ analyzer, which was disconnected from the chamber during that period.

Figure 7 shows an experiment conducted at an extremely high initial toluene/NO ratio of 136, 3800 ppb toluene and 28 ppb NO were used. As in the low-NO$_x$ experiment presented in Figure 5, the simplified simulation is able to describe the concentration–time profiles of benzaldehyde and the cresols well, no "dip" is evident in the cresol profiles. In accordance with this observation, a very low maximum NO$_3$ concentration of about 0.12 ppt is calculated, see Figure 7b. As in the preceding experiments, the concentration–time profile of OH exhibits a pronounced maximum and drops parallel to the NO$_x$ concentration.

In the experiment shown in Figure 8, the sum of the concentrations of NO and NO$_2$ was maintained at a constant level of 3–3.5 ppb. This was achieved by an automated system which added more NO when the NO$_x$ concentration reached a given minimum value. Initially, 680 ppb toluene and approximately 2.3 ppb of NO were added. The compensation for losses of NO$_x$ has the important consequence that the OH radical concentration remained at a constantly high level throughout the experiment, with no distinctive maximum observed (see Figure 8a). The simulation described the concentration–time behavior of benzaldehyde and the cresols very well. This could be expected as the NO$_x$ concentrations are even lower here than in the experiment displayed in Figure 5, the amount of NO$_2$ present is insufficient to give rise to a significant formation of NO$_3$, as evidenced by the very low maximum NO$_3$ concentration of about 0.14 ppt reached toward the end of the experiment.

The experiment shown in Figure 9 is of the same type as that shown in Figure 8, but here a somewhat higher NO$_x$ concentration of between 8.5 and 12 ppb was kept constant. As before, this leads to the OH radical concentration remaining relatively constant at around 10^7 cm^{-3} throughout the experiment (see Figure 9a). In contrast to the previous experiment, the simulation is only able to describe the concentration–time profiles of the cresols until shortly after their maxima. After this time, the decay of the cresols is significantly faster than predicted by the simplified mechanism. This discrepancy occurs at the same time when the calculated NO$_3$ radical concentration sharply rises (see Figure 9b). Toward the end of the experiment, it reaches a maximum of almost 0.9 ppt, and is thus at a level high enough to have an influence on the cresols.

The experiment displayed in Figure 10 was conducted under conditions aimed at suppressing the formation of NO$_3$ radicals as much as possible while at the same time having very high concentrations of NO$_x$. Therefore, in contrast to the experiments presented in Figures 8 and 9, where the total concentration of NO$_x$ (NO + NO$_2$) was kept constant, in this experiment the NO concentration was maintained at a constant level of 300 ppb. This extremely high NO concentration scavenged most of the ozone and virtually any NO$_3$ formed.

The concentration–time profile of OH showed a broad maximum, followed by a slow decay (see Figure 10a). This behavior can probably be attributed to increasing scavenging of OH through reaction with NO$_2$ toward the end of the experiment. As expected, only very low NO$_3$ concentrations were calculated under these conditions, the maximum is about 0.02 ppt at the end of the experiment. Consequently, the concentration–time behavior of both benzaldehyde and the cresols is described very well by the simplified simulation (see Figure 10a).

Conclusions and Implications for the Atmosphere. Ring-retaining products are formed in the photooxidation of toluene in significant yields, with *o*-cresol being the most important single compound. The individual yields determined were 5.8 ± 0.8% for benzaldehyde, 12.0 ± 1.4% for *o*-cresol, 2.7 ± 0.7% for *m*-cresol, and 3.2 ± 0.6% for *p*-cresol. The total yield of the cresol isomers is 17.9 ± 2.5%, thus they comprise a significant fraction of the overall carbon balance.

The formation of cresols in significant yields has implications for the photooxidant formation from aromatic hydrocarbons, as the cresols have a comparably low reactivity with regard to oxidant formation.[33] This is in contrast to ring-fragmentation products, some of which represent radical sources which leads to increased photooxidant formation. The formation of significant amounts of cresols is therefore expected to lessen the photooxidant formation from aromatic hydrocarbons.

Another important result of this study is the observed loss of the cresols toward the end of many experiments, which could not be explained by OH reaction alone. No such losses of benzaldehyde occurred. This and the good correlation of the losses to calculated concentration−time profiles and maximum concentrations of NO₃ radicals leads to the conclusion that reaction of the cresols with NO₃ radicals is most probably responsible for this effect. The reaction of the cresols with NO₃ is known to be considerably faster than that of benzaldehyde.[5,32] In their kinetic study of the NO₃ radical reactions with cresols, Carter et al.[34] had already suggested that this reaction can be an important atmospheric sink for cresols. The question of whether this is the case even under daylight conditions is, however, difficult to answer. For *o*-cresol, the OH reaction rate constant is about 3 times higher than the NO₃ reaction rate constant,[5,32] and it can be calculated that if the OH concentration is in the range 10^6−10^7 cm^{-3} or 0.04−0.4 ppt under typical photosmog conditions, NO₃ radical concentrations of 0.12−1.2 ppt are required for the two reactions to be competitive. Atmospheric daytime NO₃ radical concentrations are currently not known, the detection limit of even the most sensitive measurement technique currently employed is around 1 ppt at night.[35] Daytime NO₃ concentrations above the detection limit have not been observed, and estimates give upper limits lower than 1 ppt.[14] They might therefore very well be in the range where reaction of NO₃ can be a nonnegligible daytime sink for the cresols and other fast-reacting organic compounds. This may be the case in polluted situations with dense cloud cover during which photolysis rates of O₃, NO₂, and NO₃ will be low thus allowing higher steady-state concentrations of NO₃ radicals. Therefore, further investigations seem highly desirable to elucidate daytime NO₃ radical concentrations. This might be accomplished by simultaneously monitoring humidity, NO$_x$, ozone, RO₂ radicals, the spectral light distribution and intensity, and hydrocarbons which might constitute additional sinks of NO₃, downwind of a large city. With these data, daytime NO₃ concentrations may be estimated using the pseudo steady-state approximation for NO₃.

In the simulations of the experimental concentration−time profiles of benzaldehyde and the cresols obtained in this study, a "prompt" formation mechanism was assumed for these products. As evident in Figures 2−10, this mechanism was well suited to describe their formation kinetics. Attempts to reproduce the concentration−time behavior with a delayed mechanism, e.g., through further reaction of a stable intermediate, proved unsuccessful. It can therefore be concluded that the cresols are formed directly from the reaction of O₂ with the toluene−OH adduct, i.e.

$$\text{toluene−OH} + O_2 \rightarrow \text{cresol} + HO_2$$

with no stable intermediate involved.

A different formation mechanism for the cresols was recently proposed by Stockwell et al.[35] They suggested the formation of cresols from the reaction of ozone with the aromatic−OH adduct, while assuming a low yield of 2% for the cresol formation from the reaction of aromatic−OH adducts with

molecular oxygen. Stockwell et al. incorporated these pathways into their Regional Atmospheric Chemistry Model (RACM) in an attempt to reconcile the data from Bierbach et al.[9] with those of Atkinson and Aschmann.[11]

This proposed mechanism is not supported by the results of the present study, as a rapid cresol formation was observed in the early phases of the experiment, when the ozone concentration was very low. Reaction of the toluene−OH adduct with ozone can therefore not be the main source of cresols in the experiments presented in this paper. As mentioned above, the data suggest the direct formation of cresols from the reaction of the toluene−OH adduct with molecular oxygen, with no major contribution from other reactions.

In an earlier paper by Klotz et al.,[36] the possible formation of phenol through photolysis of an intermediate, benzene oxide/oxepin, was proposed for the case of benzene. Such a pathway cannot be operative in the case of toluene investigated here, as the formation yield of cresols in the photolysis of the arene oxide expected to be formed from toluene, toluene-1,2-oxide/2-methyloxepin, was found to be negligible.[17]

Apart from their formation in the photooxidation of aromatic hydrocarbons, emissions of phenol and cresols have recently been observed in the tailpipe exhaust gases from automobiles in tunnel measurements using gas chromatography[37] and the DOAS technique.[38] Therefore, to elucidate the total atmospheric burden of cresols, it will be necessary to measure such direct emissions under realistic conditions, e.g., in a traffic tunnel. To evaluate the formation of cresols from direct emissions and/or as products of the photooxidation of toluene, measurements of cresol/toluene ratios in a downtown area are also desirable. Differential optical absorption spectroscopy (DOAS) is an ideal tool for such measurements.

References and Notes

(1) Piccot, S. D.; Watson, J. J.; Jones, J. W. *J. Geophys. Res.* **1992**, *97*, 9897.

(2) Seinfeld, J. H.; Pandis, S. N. *Atmospheric Chemistry and Physics*: *From Air Pollution to Climate Change*; John Wiley & Sons Inc.: New York, 1998.

(3) *Transport and Chemical Transformation of Pollutants in the Troposphere, Vol. 3*: *Chemical Processes in Atmospheric Oxidation*; Le Bras, G., Ed.; Springer: Berlin, Germany, 1997.

(4) Derwent, R. G.; Jenkin, M. E.; Saunders, S. M. *Atmos. Environ.* **1996**, *30*, 181.

(5) Atkinson, R. *J. Phys. Chem. Ref. Data, Monograph No. 2*, **1994**.

(6) Fritz, B.; Handwerk, V.; Preidel, M.; Zellner, R. *Ber. Bunsen-Ges. Phys. Chem.* **1985**, *89*, 343.

(7) Markert, F.; Pagsberg, P. *Chem. Phys. Lett.* **1993**, *209*, 445.

(8) Knispel, R.; Koch, R.; Siese, M.; Zetzsch, C. *Ber. Bunsen-Ges. Phys. Chem.* **1990**, *94*, 1375.

(9) Bierbach, A.; Barnes, I.; Becker, K. H.; Klotz, B.; Wiesen, E. In Sixth European Symposium *Physico-Chemical Behaviour of Atmospheric Pollutants*, Angeletti, G., Restelli, G., Eds.; EC Air Pollution Research Report 50, EUR 15609/1, Brussels, Belgium, 1994; Vol. 1, pp 129−136.

(10) Seuwen, R.; Warneck, P. *Int. J. Chem. Kinet.* **1996**, *28*, 315.

(11) Atkinson, R.; Aschmann, S. M. *Int. J. Chem. Kinet.* **1994**, *26*, 929.

(12) Smith, D. F.; McIver, C. D.; Kleindienst, T. E. *J. Atmos. Chem.* **1998**, *30*, 209.

(13) Platt, U.; Perner, D.; Pätz, H. W. *J. Geophys. Res.* **1979**, *84*, 6329.

Oxidation of Toluene in an Outdoor Photoreactor

J. Phys. Chem. A, Vol. 102, No. 50, 1998 **10299**

(14) Heintz, F.; Platt, U.; Flentje, H.; Dubois, R. *J. Geophys. Res.* **1996**, *101*, 22891.

(15) Finlayson-Pitts, B. J.; Pitts, J. N., Jr. *Atmospheric Chemistry: Fundamentals and Experimental Techniques*; John Wiley & Sons: New York, 1986; Chapter 5-C.

(16) Wängberg, I.; Etzkorn, T.; Barnes, I.; Platt, U.; Becker, K. H. *J. Phys. Chem. A* **1997**, *101*, 9694.

(17) Klotz, B.; Barnes, I.; Becker, K. H. *Chem. Phys.* **1998**, *132*, 289.

(18) Trost, B.; Stutz, J.; Platt, U. *Atmos. Environ.* **1997**, *31*, 3999.

(19) Volkamer, R.; Etzkorn, T.; Geyer, A.; Platt, U. *Atmos. Environ.* **1998**, *32*, 3731.

(20) Etzkorn, T.; Klotz, B.; Sørensen, S.; Patroescu, I. V.; Barnes, I.; Becker, K. H.; Platt, U. *Atmos. Environ.*, in press.

(21) Atkinson, R.; Aschmann, S. M.; Arey, J. *Int. J. Chem. Kinet.* **1991**, *23*, 77.

(22) Atkinson, R.; Aschmann, S. M.; Arey, J.; Carter, W. P. L. *Int. J. Chem. Kinet.* **1989**, *21*, 801.

(23) *The European Photoreactor EUPHORE*; Final Report of the EC-Project, Contract EV5V-CT92-0059; Becker, K. H., Ed.; Wuppertal, Germany, 1996.

(24) Orlando, J. J.; Tyndall, G. S.; Moortgat, G. K.; Calvert, J. G. *J. Phys. Chem.* **1993**, *97*, 10996.

(25) Atkinson, R.; Carter, W. P. L.; Darnall, K. R.; Winer, A. M.; Pitts, J. N., Jr. *Int. J. Chem. Kinet.* **1980**, *12*, 779.

(26) Atkinson, R.; Carter, W. P. L.; Winer, A. M. *J. Phys. Chem.* **1983**, *87*, 1605.

(27) Shepson, P. B.; Edney, E. O.; Corse, E. W. *J. Phys. Chem.* **1984**, *88*, 4122.

(28) Bandow, H.; Washida, N.; Akimoto, H. *Bull. Chem. Soc. Jpn.* **1985**, *58*, 2531.

(29) Gery, M. W.; Fox, D. L.; Jeffries, H. E.; Stockburger, L.; Weathers, W. S. *Int. J. Chem. Kinet.* **1985**, *17*, 931.

(30) Leone, J. A.; Flagan, R. C.; Grosjean, D.; Seinfeld, J. H. *Int. J. Chem. Kinet.* **1985**, *17*, 177.

(31) Martín-Reviejo, M.; Pons, M.; Wirtz, K.; Etzkorn, T.; Senzig, J. In *The Oxidizing Capacity of the Troposphere*, EC Air Pollution Research Report 60, EUR 17482 EN, Larsen, B., Versino, B., Angeletti, G., Eds.; Luxemburg, **1997**; pp 350−354.

(32) Wayne, R. P.; Barnes, I.; Biggs, P.; Burrows, J. P.; Canosa-Mas, C. E.; Hjorth, J.; Le Bras, G.; Moortgat, G. K.; Perner, D.; Poulet, G.; Restelli, G.; Sidebottom, H. *Atmos. Environ.* **1991**, *25A*, 1.

(33) Carter, W. P. L. *J. Air Waste Manage. Assoc.* **1994**, *44*, 881.

(34) Carter, W. P. L.; Winer, A. M.; Pitts, J. N., Jr. *Environ. Sci. Technol.* **1981**, *15*, 829.

(35) Stockwell, W. R.; Kirchner, F.; Kuhn, M.; Seefeld, S. *J. Geophys. Res.* **1997**, *102*, 25847.

(36) Klotz, B.; Barnes, I.; Becker, K. H.; Golding, B. T. *J. Chem. Soc., Faraday Trans.* **1997**, *93*, 1507.

(37) Fraser, M. P.; Cass, G. R.; Simoneit, B. R. T. *Environ. Sci. Technol.* **1998**, *32*, 2051.

(38) Platt, U.; Kurtenbach, R. In *BMBF-Verbundvorhaben: Troposphärenschwerpunkt. Leitthema 3: Prozeßstudien zur Oxidantienbildung und Oxidationskapazität: Zwischenbericht*; Becker, K. H., Ed., Wuppertal, Germany, **1998**; pp 101−109.